

Influence of Sieve Trays on the Mass Transfer of Single Drops

Martin Henschke and Andreas Pfennig

Lehrstuhl für Thermische Verfahrenstechnik, RWTH Aachen, D-52056 Aachen, Germany

Mass transfer on single drops was studied experimentally in a conical glass test cell on a laboratory scale. To determine the influence of internals on the mass transfer, two different sieve trays with hole diameters of 3 and 6 mm, respectively, were inserted into the cell. In the experiments the resting times the drops stayed under and above a sieve tray were varied. Through the evaluation of the experimental results with a model, it is possible to determine the influences of the flow field and the sieve-tray passage on mass transfer separately. The mixing inside the drops while they passed through the holes is relatively small even if the drops are a little larger than the hole diameter. The influence of changes of the flow field caused by the sieve trays on mass transfer is larger, and its quantitative magnitude depends on the system used.

Introduction

Today, for the safe design of technical liquid–liquid extraction columns, experiments on a pilot-plant scale are unavoidable (Schröter et al., 1998). These experiments are time-consuming and expensive for the industry. Thus, our long-term goal is to replace the pilot-plant experiments by a design technique that is based only on simulations and laboratory-scale test-cell studies.

In this context the mass transfer that occurs in an extraction column is of major importance. For the experimental study of mass transfer and for the determination of overall mass-transfer coefficients laboratory-scale test cells have been used for a long time. Mostly, these test cells are glass tubes with a length of up to 1.5 m in which rising drops are investigated (Garner et al., 1959; Garner and Tayeban, 1960; Johnson and Hamielec, 1960; Skelland and Wellek, 1964; Liang and Slater, 1990; Slater, 1995; Temos et al., 1996). However, conical test cells, in which the drops are suspended in a counter-current flow, are also used (Otto et al., 1973; Modigell, 1981; Schröter et al., 1998; Henschke and Pfennig, 1999). Since all of these studies were performed without internals in the test cell, the results can be transferred only to spray columns, because the internals improve the mass transfer in columns.

In order to obtain quantitative information on the influence of internals, in recent studies a single sieve tray has been inserted into a 0.4 to 0.8 m high glass tube in which the drops

were rising. With this experimental setup, overall mass-transfer coefficients were determined and transferred to sieve-tray columns (Qi, 1992; Hoting and Vogelpohl, 1993; Wagner, 1999; Qi et al., 2000). In some cases, but unfortunately not in all, this procedure was successful, and the mass transfer in a column could be predicted. As a reason for the partly bad correspondence between the single-drop experiments and the column results, Wagner (1999) indicated the different residence times in the two devices. Accordingly it is necessary to consider the sieve-tray influence not only lumped into an overall mass-transfer coefficient, but to quantify the influence in more detail. This has been achieved in this work by mass-transfer measurements of single drops with varying residence times below and above a sieve-tray.

It should be possible to transfer the results represented in the following to technical columns with dual-flow trays operating in the dispersion regime, if the system is coalescence-inhibited and the drop breakage essentially takes place within a comparatively short inlet region of the column. The results cannot be applied to columns with flow slots operating in the mixer–settler regime.

Experimental Section

Setup of the test cell

The mass-transfer experiments were carried out on a laboratory scale in a conical glass test cell. The test cell, with its major dimensions, is shown in Figure 1. It can be used either

Correspondence concerning this article should be addressed to A. Pfennig.

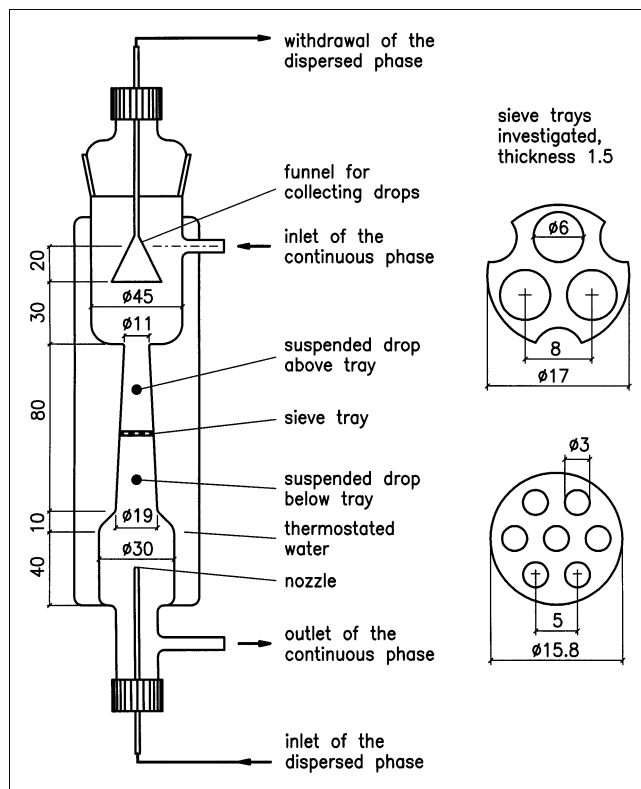


Figure 1. Mass-transfer cell.

All measures are given in mm.

with or without one of the shown sieve trays (6- or 3-mm hole diameter). During the experiments the following cycle will be performed for each drop in a series of measurements:

1. The countercurrent flow of the continuous phase is turned off. A Hamilton precision-syringe drive (type Micro-lab M) pumps a previously specified liquid volume into the drop-generation nozzle and a drop is formed. When the drive stops, the drop detaches from the nozzle and starts to rise. (For the generation of different drop sizes, different nozzles are necessary.)

2. When the drop has risen to about 15 mm below the sieve tray, the countercurrent flow is switched on. The flow rate is adjusted such that the drop neither touches the sieve tray nor is flushed out of the test cell toward the bottom.

3. After a predefined time the countercurrent flow is turned off for 0.5 to 1 s. Thus, the drop rises and passes a hole in the sieve tray.

4. Now the countercurrent flow is switched on again and the drop stays above the sieve tray.

5. After a second specified time period, the countercurrent flow is turned off again and the drop rises into the funnel. There it coalesces quickly at a Teflon tip (coalescence aid) and is withdrawn by a second precision-syringe drive.

If the test cell is used without a sieve tray, steps 2 and 3 are omitted, and the drops are suspended at a constant height within the cell. Preliminary investigations have shown that the mass transfer is not much affected by variation in the vertical position of the drops in the conical part of the cell. After collecting approximately 20 to 150 drops (depending on

the drop size, the sample should be about 1 mL) the drop phase is analyzed.

All parts of the test cell that come into contact with the system are made of glass, stainless steel, or PTFE. The continuous phase is pumped with a gearwheel pump (Verder, type V108.05) with stepless speed control by a frequency converter (Lenze, type 8201E). The flow rate is measured with a flowmeter from Bopp & Reuther (type BGN-120(I)-15-100-E2). Before the experiments, it is calibrated with the continuous phase by weighting the amount of liquid that was pumped for a specified period. Thus, a precision of ± 0.2 L/h is reached. The temperature is adjusted by external water circulation. The water flows through cooling jackets around the reservoir and the test cell as well as the cooler for the continuous phase, which is placed between the pump and the test cell. The water temperature is controlled ($\pm 0.1^\circ\text{C}$) by a thermostat from Lauda (type NB-S15/12).

The operation of the syringe drives and the pump for the countercurrent flow is controlled by a personal computer with the software Visual Designer from Intelligent Instrumentation.

Systems used and operating conditions

In the experiments, two standard test systems proposed by the EFCE (Misek et al., 1985) were used. These were toluene/acetone/water and *n*-butyl acetate/acetone/water. The drops always consisted of the organic phase, which was saturated with water. The drop diameters were $3.22 (\pm 0.05)$ mm and $3.06 (\pm 0.05)$ mm for the toluene and the *n*-butyl acetate drops, respectively. The dosage of the drop volumes was done by using a 2.5 mL Hamilton syringe (type 1002 TLL) and a syringe-drive velocity of 7 s per stroke for the toluene system and 10 s per stroke for the *n*-butyl acetate system. Thus, the drop formation time is 49 ms and 60 ms for the toluene drops and the *n*-butyl acetate drops, respectively.

The continuous phase consisted of water with 4–5 wt% acetone (solute), and was saturated with the organic solvent after the acetone addition. The water used was first deionized and then distilled. The solvents were obtained from Merck KG and were of the purity p.a. (toluene) and “reinst” (*n*-butyl acetate and acetone). The experiments were carried out at $20^\circ\text{C} (\pm 0.1)$ and ambient pressure. A listing of the series of experiments performed is presented in Table 1.

Table 1. Experiments Performed*

Ser.	Org. Phase	d_L (mm)	\dot{V}_u (L/h)	t_u (s)	t_h (s)	\dot{V}_o (L/h)	t_o (s)	t_K (s)	x_α (wt. %)
1	Butyl ac.	3	30	0.5–4.2	1.0	30	4.5–0.8	6.0	4.4
2	Toluene	3	30	0.5–4.3	0.7	30	4.8–1.0	6.0	4.8
3	Toluene	3	30	0.5–10.0	0.8	30	10.7–1.2	12.0	4.7
4	Toluene	6	50	0.5–4.2	0.7	30	4.8–1.1	6.0	4.5
5	Toluene	3	15–50	4.3	0.6	30	1.1	6.0	4.7
6	Toluene	6	20–70	4.2	0.7	30	1.1	6.0	4.5

* d_L : hole diameter of the sieve tray; \dot{V}_u , \dot{V}_o : volume flow rates in the cell for drops underneath/above the tray; t_u , t_o : residence times for drops underneath/above the tray; t_h : time the countercurrent flow is shut off (drops pass the hole); t_K : entire residence times in the cell; x_α : concentration in the continuous phase.

Analytical methods

The acetone concentration in the toluene sample was determined by gas chromatography. A gas chromatograph from Siemens-type Sichromat and a fused-silica capillary column from Macherey-Nagel, type Optima 1-DF-5 (injecting-block temperature: 250°C; column temperature: 60°C) were used. For detection a built-in FID was used at 250°C. The measured signal was evaluated with an integrator from Shimadzu, type C-R3A. Methyl ethyl ketone was used as the internal standard. In the range between 0.25 and 8 wt.% of acetone, the average relative error is 1.1%.

The acetone concentration in the *n*-butyl acetate sample was determined with a two-beam UV/VIS spectrometer (Lambda 2 from Perkin-Elmer) and quartz-glass cells with 2-mm layer thickness (Hellma, type Suprasil No. 110-QS) at a temperature of 30°C. The spectra were evaluated at 270 nm and a reference point at 320 nm. The average relative error determined from the calibration data is 0.2%.

To determine the concentration of the organic phase in equilibrium with the continuous aqueous phase, a sample of the organic phase was withdrawn every day from the reservoir, where it has been added for the saturation of the aqueous phase, and was analyzed. The acetone concentration in the aqueous phase indicated in Table 1 was calculated from the measured concentration in the organic phase based on the available equilibrium data (Misek et al., 1985).

Theory

In the experiments, the residence time of the drops in the cell is short as compared to the time necessary for equilibration. Thus, the mass transfer between the drops and the continuous phase is not in steady state and cannot be described with a constant mass-transfer coefficient inside the drop. Nevertheless, in the literature a constant mass-transfer coefficient is frequently assumed and the initially increased mass-transfer rate is taken into consideration either by an adapted initial concentration or by an adapted residence time (Qi, 1992; Skelland and Wellek, 1964). In the sense of modeling as exactly as possible, it is, however, better to do the calculations with an unstationary model (Steiner, 1986). This can be done relatively simply, for in the past it has been shown repeatedly that an effective or eddy diffusion coefficient in the drop can be assumed to be constant with time (Johnson and Hamielec, 1960; Boyadzhiev et al., 1969; Steiner, 1986; Slater and Hughes, 1993; Slater, 1995). In this case, the molecular diffusion coefficient is multiplied by an enhancement factor *E* to obtain the effective diffusion coefficient

$$D_{\text{eff}} = ED_d \quad (1)$$

This equation is valid only for a specific drop diameter, *d*, because in general *E* depends on *d* (Wagner, 1999). Except for this restriction the range of applicability of Eq. 1 is very wide, for example, the circulation inside a drop that is induced hydrodynamically by the sedimentation can be taken into account with *E* = 2.5, if the convection is fast as compared to the diffusion. Then a separate consideration of convection terms is not necessary (Kronig and Brink, 1950; Johns and Beckmann, 1966; Brauer, 1979; Brander and Brauer, 1993). Also, interphase instabilities such as eruptions or

Marangoni circulations can be described satisfactorily. In this case *E* can reach values of 50 or even more (Johnson and Hamielec, 1960; Davies, 1972). Equation 1 can be used in connection with a model of Newmann (1931) to obtain the time-dependent concentration change in a drop

$$\frac{y(t) - y_\alpha}{y_I - y_\alpha} = 1 - \frac{6}{\pi^2} \sum_{j=1}^{\infty} \frac{1}{j^2} \exp[-(j\pi)^2 Fo] \quad (2)$$

with

$$Fo = \frac{4ED_d t}{d^2} \quad (3)$$

Here, *y_I* is the concentration inside a drop directly at the interphase. If the mass-transfer resistance outside the drop is negligible, *y_I* is in equilibrium with the bulk continuous phase

$$y_I = kx_\alpha \quad (4)$$

Instead of the series expansion from Newman (Eq. 2), different, faster converging series expansions, for example, from Steiner (1986) or Kronig and Brink (1950), can be used. Also numeric procedures (Olander, 1966) or formulations with the error function (Mersmann, 1986) are well known. As expected from a mathematically accurate description, the results are the same in all cases, if the same definition of the *Fo* number is used and a sufficiently large number of series members or a sufficient numeric accuracy is considered.

The preceding discussion considers only the dispersed phase. The continuous phase near the drop surface is replaced continually due to drop sedimentation. Therefore, a concentration boundary layer cannot build up continually, as inside the drop, where it finally reaches the center. Rather a constant boundary-layer thickness will be developed after the first few milliseconds of drop formation. In this case, modeling of the outside mass transfer is possible with a constant mass-transfer coefficient, *β_c*. However, the question is how this mass-transfer coefficient can be calculated. In the generally applied equations, for example, according to Mersmann (1986), only the diffusion coefficient *D_c* of the continuous phase without an enhancement factor is implemented

$$\beta_c = \sqrt{\frac{4v_\infty D_c}{\pi d}} f(Re, \eta_d/\eta_c) \quad (5)$$

If *E* is very large in the dispersed phase, convections at the interface are most likely to occur, which would improve the mass transfer in the continuous phase, too. Thus, it is problematic to use Eq. 5 in the continuous and Eq. 1 in the dispersed phase. Fortunately for both systems investigated here the mass-transfer resistance outside the drop is small compared to the resistance inside the drop (Henschke and Pfennig, 1999). Correspondingly, only the mass-transfer resistance inside the drop is considered in the following. For the outside of the drop it is assumed: *x* = *x_α* = const.

In spite of this simplification the evaluation of the single-drop experiments is not simple, because there are two effects increasing mass transfer that don't occur in experiments with-

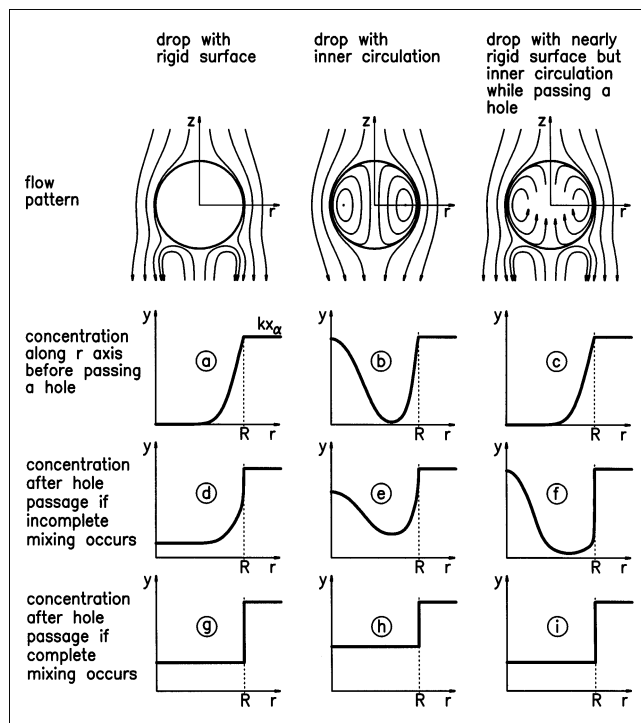


Figure 2. Concentration in a drop before and after passing a hole.

out a sieve tray. On the one hand, the flow field is more inhomogeneous underneath the sieve tray than above it. This becomes apparent through the “dancing” of the drops, and in the modeling it is also accounted for by the enhancement factor, that is, E_u (under the tray) is larger than E_o (above the tray). On the other hand, by the passing through the hole (hole passage) the fluid inside the drop may be more or less completely mixed. The mixing will partly destroy the concentration boundary layer.

In Figure 2 possible concentration profiles in the equatorial plane of drops are shown for three characteristic cases. Profiles (a) to (c) correspond to drops under the sieve tray, while (d) to (i) represent drops after a hole passage. During the residence time below a sieve tray, a drop with a rigid interface develops an approximately spherical symmetrical concentration profile. During the hole passage, the drop is deformed depending on the d/d_L ratio. This deformation causes a more or less complete mixing inside the drop. If the mixing is complete [concentration profile (g) in Figure 2], the entire mass transfer under and above the sieve tray can be calculated using Eq. 2. First Eq. 2 is evaluated, with $t = t_u$ and $y_a = 0$ to get $y_u(t_u)$. Next Eq. 2 is evaluated once again, with $t = t_o$ and $y_a = y_u$ to get the average concentration $y(t_u + t_o)$ of the drops after the entire residence time in the cell.

If the drop develops an inner circulation, a rotationally symmetrical concentration profile around the z -axis is formed. Again the mixing during the hole passage will be more or less intense. The mathematical description in the limit of complete mixing [(h) in Figure 2] is possible in the same way as described earlier if E_u and E_o are increased to appropriately account for the circulation.

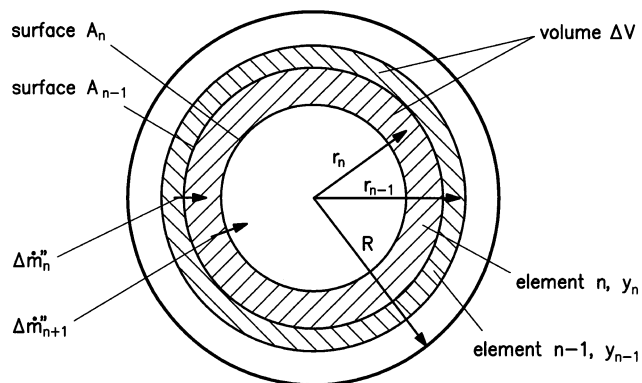


Figure 3. Definition of the volume elements for numerical calculations.

Finally, a drop with a rigid interface is conceivable in which the inner circulation is induced only during the hole passage due to the increased shear stress. In an extreme case it may happen that most of the concentration boundary layer is displaced to the drop center [(f) in Figure 2]. As a result, the drop would have an even better mass transfer above the hole than it would have in the case of complete mixing [(i) in Figure 2]. In the case of complete mixing by the hole passage, mass transfer can be modeled the same way as discussed for the drop with a rigid interface.

As shown in the last paragraphs, modeling of the mass transfer in the case of complete mixing upon hole passage can be achieved even for different flow characteristics. But the analytical modeling of incomplete mixing is not possible with the available equations. Thus, evaluation of the experimental data was done numerically by solving the appropriate differential equations. The division of a drop into N volume elements is shown in Figure 3. Each element has the same volume ΔV

$$\Delta V = \frac{V}{N} = \frac{\pi d^3}{6N} \quad (6)$$

The radius r_n of the geometrical center of each element is

$$r_n = \sqrt[3]{\frac{3(V - (n - 0.5)\Delta V)}{4\pi}} \quad \text{for } n = 1 \dots N \quad (7)$$

The surface area of each element is therefore

$$A_n = \pi \left[2 \left(\frac{3(V - n\Delta V)}{4\pi} \right)^{1/3} \right]^2 \quad (8)$$

Now the time-dependent mass flux per unit area can be calculated using Fick's law in connection with Eq. 1. It is assumed that the diffusive mass flux is sufficiently small and causes no noticeable convection flux (Baehr and Stephan, 1994). Furthermore it is assumed that the density is independent of time and concentration, and thus

$$\Delta \dot{m}''_n(t) = \rho_d D_{\text{eff}} \frac{y_{n-1}(t) - y_n(t)}{r_{n-1} - r_n} \quad (9)$$

with

$$D_{\text{eff}} = E_u D_d \quad \text{for the drop below sieve tray} \quad (10a)$$

$$D_{\text{eff}} = E_o D_d \quad \text{for the drop above sieve tray.} \quad (10b)$$

In the calculations, Eq. 9 is first evaluated for all elements $n = 1$ to N . Then the new concentration in each element is calculated from

$$y_n(t + \Delta t) = y_n(t) + (\Delta \dot{m}_n'' A_{n-1} - \Delta \dot{m}_{n+1}'' A_n) \Delta t / \Delta V. \quad (11)$$

It is to be noted that $A_N = 0$. For a complete description of the problem, the initial conditions and the boundary conditions for the hole passage have to be defined. At the drop surface ($n = 0$, $r_0 = d/2$) equilibrium with the continuous phase is assumed at any time, as just discussed

$$y_0 = kx_\alpha. \quad (12)$$

Since initially the drop phase doesn't contain any acetone and the drop formation time is very short, no initial concentration is considered inside the drop

$$y_n(t = 0) = 0 \quad \text{for } n = 1 \dots N. \quad (13)$$

For the hole passage a partial mixing inside the drop is taken into account by calculating a weighted average between the concentration profile immediately before the hole passage and the mean concentration in the drop. The calculation is performed with a dimensionless weighting parameter Ω

$$y_n|_{\text{after hole passage}} = \Omega \bar{y} + (1 - \Omega) y_n|_{\text{before hole passage}}, \quad (14)$$

with

$$\bar{y} = \frac{1}{N} \sum_{n=1}^N y_n|_{\text{before hole passage}}. \quad (15)$$

This modeling does not include case (f) in Figure 2. In all other cases, this type of interpolation appears to be appropriate.

For the numerical calculations the number of the elements, N , and the time period, Δt , are chosen. If $N = 20$ and $\Delta t = 0.002$ s, the difference between the numerical result achieved without sieve-tray passage and the theoretical solution from Eq. 2 is only 1% at a simulation time of 1 s. For longer simulation times, the result is even better.

Since we only account for Fickian diffusion and do not consider convective mass transfer inside the drop, we expect to obtain an enhancement factor that includes the effect of internal circulation.

In order to depict drop movement appropriately in the model, the drop passage time, t_h , (Table 1) has to be accounted for in the calculations. The time period, t_h , during which the countercurrent flow in the test cell is turned off lies between 0.7 and 1.0 s. The drop does not require the entire time, t_h , for the hole passage, since it first rises about 15 mm to the sieve tray, then slips through a hole, and finally

risers a further 15 mm until the countercurrent flow is switched on again. Accordingly for the toluene drops, which have a terminal velocity of 86 mm/s, the time they remain below (t_u) and above (t_o) the sieve tray increases by 0.17 s each. The terminal velocity of the *n*-butyl acetate drops is 78 mm/s. Thus 0.19 s are added to t_u and t_o . The residual time of the hole passage ($t_h - 0.34$ s and $t_h - 0.38$ s, respectively) is considered only implicitly in the calculation, since it is accounted for in the mixing parameter, Ω .

Results and Discussion

In Figure 4 the experimental results of series 2 are presented together with the model computations. The model parameters E_u , E_o , and Ω are obtained by least-square fitting to the experimental data. At the time $t = 0$ the dimensionless concentration difference is unity. As time passes, the concentration difference is reduced by mass transfer. As long as a drop is suspended underneath the sieve tray, the decrease follows the continuous line that was computed with an enhancement factor that was fitted to be $E_u = 32.9$. The time it takes to pass through the sieve tray is characterized by an open circle in the diagram. At this time the mixing in the drop is calculated using $\Omega = 0.20$ in Eq. 14. After the passage, the mass transfer follows one of the dashed lines that are calculated with $E_o = 12.5$. After about 6 s, the drops were withdrawn and analyzed. The results are shown as filled circles in Figure 4. The fitted values of the enhancement factors show that E_u is 2.6 times larger than E_o . This might be due to the comparably unsteady flow underneath the sieve tray that leads to the "dancing" of the drops, as already stated. The small value, 0.2, of the mixing parameter, Ω , is amazing. Although the 3-mm holes of the sieve tray are slightly smaller than the 3.22-mm drops, which are thus deformed during the hole passage, about 80% of the concentration profile are maintained and only 20% are mixed.

Thus the major effect of the sieve trays is not the mixing inside the drops during the hole passage but rather to induce a strongly inhomogeneous flow pattern that enhances mass

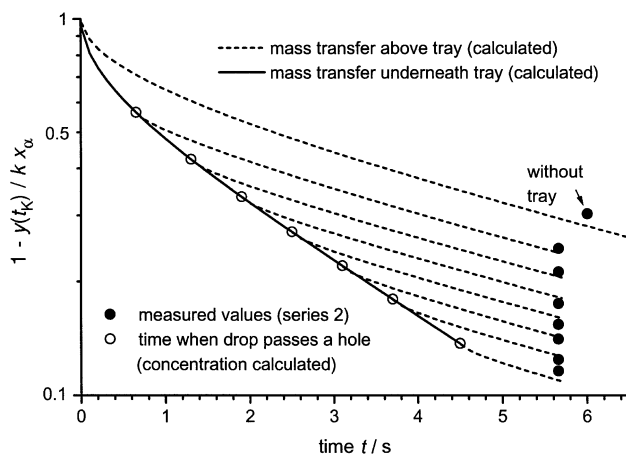


Figure 4. Influence of the residence time underneath a sieve tray on the mass transfer.

Experimental data: series 2, toluene drops ($d = 3.22$ mm) in water, mass transfer (acetone) into the drops.

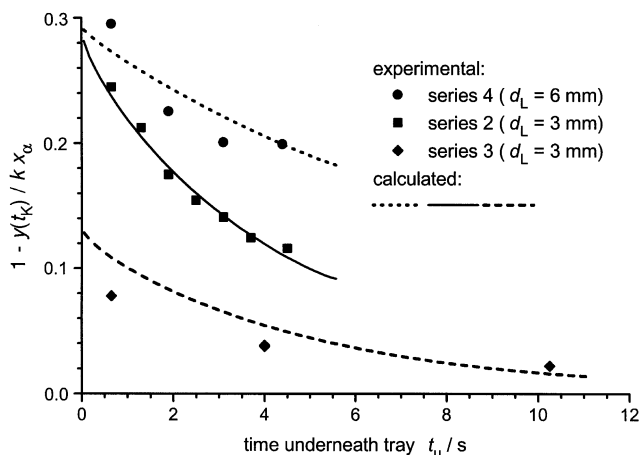


Figure 5. Influence of the residence time and the sieve-tray geometry on the mass transfer.

Toluene drops ($d = 3.22$ mm) in water, mass transfer (acetone) into the drops. Sieve trays with hole diameters of $d_L = 3$ mm and $d_L = 6$ mm, respectively.

transfer. Also Slater et al. (1988) reported that mass transfer was not increased in rising drops that were deformed while passing through the Raschig rings. Slater et al., however, did not distinguish between flow and the deformation influences. Thus, interpretation of their results is difficult.

In test series 2, 3, and 4, shown in Figure 5, the hole diameter and the residence time in the test cell vary. On the x -axis, only the residence time underneath the sieve tray, t_u is plotted, while the dimensionless concentrations on the y -axis still correspond to t_K . Comparing series 2 ($d_L = 3$ mm) with series 4 ($d_L = 6$ mm) shows that the deviation between the experimental data increases with increasing time, t_u . There are two physical explanations for this behavior. On the one hand, the flow in the holes gets faster as the free area of the tray decreases and as a result of this the roughness of the flow under the tray, and thus E_u , increases. It may be assumed that this can be described by an empirical approach like

$$E_u = \frac{E_o}{\Phi^\kappa}, \quad (16)$$

where Φ is the ratio of the hole area to the total area of the sieve tray. On the other hand, the mixing parameter Ω decreases with increasing hole diameter at constant drop diameter, since the drop deformation and the shear forces at the drop surface will decrease. A possible way to describe this dependency in an empirical function is

$$\Omega = \exp\left(\lambda \frac{d_L}{d}\right), \quad \lambda < 0. \quad (17)$$

With Eqs. 16 and 17, only three parameters for modeling (E_o , κ , λ), with which all experiments with the toluene system were fitted simultaneously, are still necessary. The result of the least-square fitting is $E_o = 12.5$, $\kappa = 0.71$, and $\lambda = -1.5$. Calculating the mixing parameter from these results for the sieve tray with a 6-mm hole diameter, yields $\Omega = 0.06$.

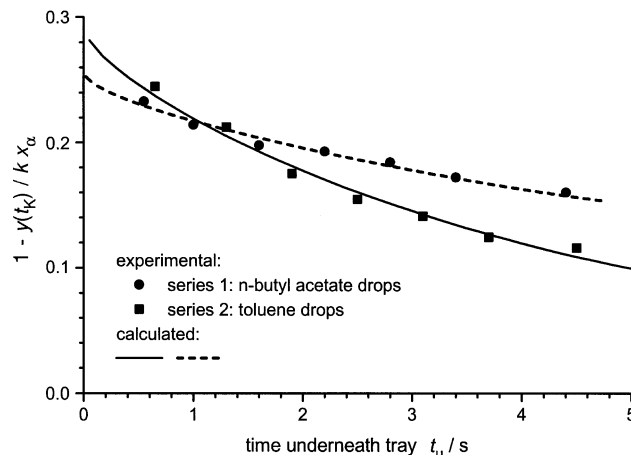


Figure 6. Dependency of the mass transfer on the system used.

Series 1: *n*-butyl acetate drops ($d = 3.06$ mm) in water. Series 2: toluene drops ($d = 3.22$ mm) in water. Mass transfer (acetone) into the drops.

Thus, the mixing is hardly noticeable. Also, the enhancement factor below the tray with 6-mm holes is only 1.6 times larger (calculated from κ) than the one above the tray. Due to Eq. 16, this result comes from smaller flow-field disturbances underneath the tray with 6-mm holes in comparison to the ones under the tray with 3-mm holes. Since the Eqs. 16 and 17 are purely empirical, they cannot describe the complex flow conditions accurately, and so they can be regarded as somewhat speculative. Nevertheless, they suggest a possible emphasis for further theoretical investigations.

The influence of the system on the mass transfer is shown in Figure 6. Because the investigations of the *n*-butyl acetate system were performed only with the tray with 3-mm hole diameter, the parameters E_u , E_o , and Ω were fitted. The result is $E_u = 27.4$, $E_o = 16.8$, and $\Omega = 0.230$. The value of Ω corresponds to $\lambda = -1.5$. Thus, the mixing can be described with the same parameter in both systems. For the *n*-butyl acetate system the enhancement factor below the tray is only 63% larger than the one above (160% for the toluene system). A possible reason may be that the *n*-butyl acetate drops always have a movable interface, while the toluene drops have a rather rigid interface above the sieve tray and a more movable one below it. This explanation is supported at least for the range above the sieve tray, where the flow is hardly affected by the tray, according to single-drop rising experiments from Haverland (1988) and Hoting (1996). The experimental sedimentation data of the toluene drops can be described with the equations for rigid spheres, while *n*-butyl acetate drops are faster as comparable spheres.

The previous results show that the enhancement factor strongly depends on the hydrodynamic details. A change in the hydrodynamics in the test cell is not only possible by an exchange of the sieve tray but also by varying of the volume flow rate in the cell. Corresponding results are shown in Figure 7. On the x -axis the ratio of the hole velocity ($v_L = \dot{V}_u/A_{\text{Holes}}$) to the sedimentation velocity of the toluene drops ($v_\infty = 86$ mm/s) is plotted. For a specific sieve tray the hole velocity is proportional to the volume flow rate. It can be

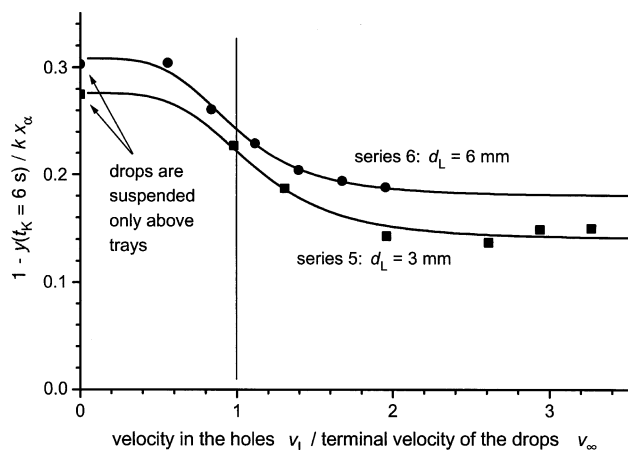


Figure 7. Influence of the sieve-tray geometry and the flow rate of the continuous phase on the mass transfer.

Toluene drops ($d = 3.22$ mm) in water; mass transfer (acetone) into the drops. Sieve trays with hole diameters of $d_L = 3$ mm and $d_L = 6$ mm, respectively.

seen that mass transfer increases with increasing hole velocity in the range of $v_L/v_\infty = 1$ for both of the sieve trays investigated. No further improvement can be observed beyond approximately $v_L/v_\infty = 1.5$. In the data even a slight reduction in mass-transfer rate can be noticed from $v_L/v_\infty \approx 3$ upwards. This is probably due to the increasing distance between the suspended drops and the sieve tray (up to 40 mm, resulting from the increasing countercurrent velocity) and the homogenization of the flow field that accompanies it. For the enhancement factor, E_u , underneath the tray these results show, that basically the flow velocity, the free area, and the distance from the tray should be considered in Eq. 16. Here further investigations are necessary.

Conclusions

In order to reach the long-term goal—a column design based only on laboratory-scale experiments—the influence of internals must be exactly quantifiable. Using the conical test cell used in this work, it is possible to obtain detailed information on various influences on mass transfer. For different sieve trays inserted in the cell, it was shown that the mass transfer was improved by both the change in the flow field caused by the trays as well as the hole passage of the drops.

The influence of the flow field on mass transfer varies depending on the system used. This probably is due to the different system-dependent mobility of the interface between the drops and the continuous phase. As expected, the improvement in mass transfer by the hole passage of a drop depends on the ratio of hole to drop diameter. However, the mixing inside the drops is relatively slight, even if the drops are a little larger than the hole. Thus, the effect of the hydrodynamic state on mass transfer is clearly more important than the effect of the hole passage. This should be taken into account in future models for extraction columns.

Acknowledgments

Parts of the work were supported by BASF AG, Bayer AG, Degussa AG, Phenolchemie GmbH, QVF Glastechnik GmbH, and

Schott Engineering GmbH. The authors also thank Mr. Jürgen Rohjahn for the conscientious realization of most of the experiments.

Notation

A = area, m^2
 d = diameter, m
 D = diffusion coefficient, m^2/s
 E = enhancement factor
 Fo = Fourier number
 k = distribution coefficient
 \dot{m}'' = mass flux per unit area, $kg/(m^2 \cdot s)$
 N = number of elements
 r = radius, m
 Re = Reynolds number
 t = time, s
 v = drop velocity, m/s
 V = volume, m^3
 \dot{V} = volume flow, m^3/s
 x = mass fraction in the continuous phase
 y = mass fraction in the drop
 z = z-axis, m

Greek Letters

β = mass-transfer coefficient, m/s
 Φ = fraction of hole area of the tray
 η = viscosity, $Pa \cdot s$
 κ = defined by Eq. 16
 λ = defined by Eq. 17
 Ω = mixing parameter
 ρ = density, kg/m^3

Subscripts

c = continuous phase
 d = dispersed phase
 eff = effective
 h = hole passage
 K = overall residence time
 L = hole of the sieve tray
 o = above tray
 u = underneath tray
 ∞ = infinitely extended fluid
 α = start up

Literature Cited

- Baehr, H. D., and K. Stephan, "Wärme und Stoffübertragung," Springer-Verlag, Berlin (1994).
 Boyadzhiev, L., D. Elenkov, and G. Kyuchukov, "On Liquid-Liquid Mass Transfer Inside Drops in a Turbulent Flow Field," *Can. J. Chem. Eng.*, **47**, 42 (1969).
 Brander, B. and H. Brauer, "Impuls- und Stofftransport durch die Phasengrenzfläche von kugelförmigen fluiden Partikeln," *Fortschr.-Ber. VDI*, No. 326, ser. 3, VDI-Verlag, Düsseldorf (1993).
 Brauer, H., "Particle/Fluid Transport Processes," *Fortschr. Verfahrenstech.*, **17**, 61 (1979).
 Davies, J. T., *Turbulence Phenomena*, Academic Press, New York (1972).
 Garner, F. H., A. Foord, and M. Tayeban, "Mass Transfer from Circulating Liquid Drops," *J. Appl. Chem.*, **9**, 315 (1959).
 Garner, F. H., and M. Tayeban, "The Importance of the Wake in Mass Transfer from Both Continuous and Dispersed Phase Systems, Part I," *An. Fis. Quim.*, **56b**, 479 (1960).
 Haverland, H., *Untersuchungen zur Tropfendispergierung in flüssigkeitspulsierten Siebboden-Extraktionskolonnen*, PhD Thesis, Technische Universität Clausthal, Clausthal-Zellerfeld, Germany (1988).
 Henschke, M., and A. Pfennig, "Mass-Transfer Enhancement in Single-Drop Extraction Experiments," *AIChE J.*, **45**, 2079 (1999).
 Hoting, B., "Untersuchung zur Fluidynamik und Stoffübertragung in Extraktionskolonnen mit strukturierten Packungen," *Fortschr.-Ber. VDI*, No. 439, Ser. 3, VDI-Verlag, Düsseldorf (1996).

- Hoting, B., and A. Vogelpohl, "Determination of Single Drop Mass Transfer Coefficients in a Laboratory-Scale Standard Apparatus," *Proc. ISEC '93*, York, England (1993).
- Johns, L. E., and R. B. Beckmann, "Mechanism of Dispersed-Phase Mass Transfer in Viscous, Single-Drop Extraction Systems," *AIChE J.*, **12**, 10 (1966).
- Johnson, A. I., and A. E. Hamielec, "Mass Transfer Inside Drops," *AIChE J.*, **6**, 145 (1960).
- Kronig, R., and J. C. Brink, "On the Theory of Extraction from Falling Droplets," *Appl. Sci. Res.*, **A2**, 142 (1950).
- Liang, T.-B., and M. J. Slater, "Liquid-Liquid Extraction Drop Formation: Mass Transfer and the Influence of Surfactant," *Chem. Eng. Sci.*, **45**, 97 (1990).
- Mersmann, A., *Stoffübertragung*, Springer-Verlag, Berlin (1986).
- Misek, T., R. Berger, and J. Schröter, *Standard Test Systems for Liquid Extraction*, 2nd ed., EFCE Publications Series No. 46, The Institution of Chemical Engineers, Warwickshire, England (1985).
- Modigell, M., *Untersuchung der Stoffübertragung zwischen zwei Flüssigkeiten unter Berücksichtigung von Grenzflächenphänomenen*, PhD Thesis, RWTH-Aachen, Aachen, Germany (1981).
- Newman, A.B., "The Drying of Porous Solids: Diffusion Calculation," *Trans. AIChE*, **27**, 310 (1931).
- Olander, D. R., "The Handlos-Baron Drop Extraction Model," *AIChE J.*, **12**, 1018 (1966).
- Otto, W., R. Streicher, and K. Schügerl, "Influence of Surface Active Agents on the Mass Transfer Across Liquid-Liquid Interfaces—I. Dioxane-Toluene-Water-System," *Chem. Eng. Sci.*, **28**, 1777 (1973).
- Qi, M., *Untersuchungen zum Stoffaustausch am Einzeltropfen in flüssigkeitspulsierten Siebboden-Extraktionskolonnen*, PhD Thesis, Technische Universität Clausthal, Clausthal-Zellerfeld, Germany (1992).
- Qi, M., H. Haverland, and A. Vogelpohl, "Auslegung von pulsierten Siebboden- und Sprühkolonnen für die Extraktion auf der Basis von Einzeltropfenuntersuchungen," *Chem. Ing. Tech.*, **72**, 203 (2000).
- Schröter, J., W. Bäcker, and M. J. Hampe, "Stoffaustauschmessungen an Einzeltropfen und an Tropfenschwärmen in einer Gegenstromzelle," *Chem. Ing. Tech.*, **70**, 279 (1998).
- Skelland, A. H. P., and R. M. Wellek, "Resistance to Mass Transfer Inside Droplets," *AIChE J.*, **10**, 491 (1964).
- Slater, M. J., "A Combined Model of Mass Transfer Coefficients For Contaminated Drop Liquid-Liquid Systems," *Can. J. Chem. Eng.*, **73**, 462 (1995).
- Slater, M. J., and K. C. Hughes, "The Application of a New Combined Film Mass Transfer Coefficient Model to the n-Butanol/Succinic Acid/Water System," *Proc. ISEC '93*, York, England (1993).
- Slater, M. J., M. H. I. Baird, and T.-B. Liang, "Drop Phase Mass Transfer Coefficients for Liquid-Liquid Systems and the Influence of Packings," *Chem. Eng. Sci.*, **43**, 233 (1988).
- Steiner, L., "Mass Transfer Rates From Single Drops and Drop Swarms," *Chem. Eng. Sci.*, **41**, 1979 (1986).
- Temos, J., H. R. C. Pratt, and G. W. Stevens, "Mass Transfer To Freely-Moving Drops," *Chem. Eng. Sci.*, **51**, 27 (1996).
- Wagner, I., *Der Einfluß der Viskosität auf den Stoffübergang in Flüssig-flüssig-Extraktionskolonnen*, Hieronymus-Verlag, München (1999).

Manuscript received Mar. 9, 2001, and revision received July 30, 2001.